

A CLASSICAL ELECTRON-CYCLOTRON MASER WITH AXIAL ELECTRON BEAM INJECTION

J. L. Vomvoridis  
Western Research Corporation  
1901 N. Ft. Myer Drive  
Arlington, VA 22209

It is shown that the Electron-Cyclotron Maser interaction can be made compatible with exclusively axial injection of the electron beam, by introducing an appropriate slow-wave structure. With an appropriate choice for the relevant parameters, the resulting interaction is found to be extremely efficient, with efficiencies approaching 100 percent, and to possess a moderate frequency upshift from the non-relativistic gyrofrequency. The nonlinear theory of the interaction is outlined and preliminary designs are presented.

Introduction

In the Electron-Cyclotron Maser (ECM) interaction,<sup>1-3</sup> an electron beam propagates along a magnetostatic field and interacts with an electromagnetic wave with transverse electric field polarization. For this interaction, the frequency is approximately equal to the relativistic electron gyrofrequency in the magnetostatic field. The principal experimental realization of the ECM is the gyrotron,<sup>4-6</sup> in which the electromagnetic wave propagates essentially at a right angle to the magnetostatic field. The gyrotron has a prevalent position among microwave generators for its distinct features of high efficiency (~40 percent) and short wavelength operation, below 1 cm. In the gyrotron, the electron beam energy available to the interaction is that associated with the gyrating motion of the electrons, while the axial electron velocity remains largely unaffected by the interaction. However, large values of the pitch angle must be avoided, since they introduce a large thermal spread in the axial velocity and destroy the resonance.

It is therefore very important to identify an interaction which combines attractive features of the gyrotron (high efficiency and frequency) with exclusively axial injection of the beam. The purpose of this letter is to show that such an interaction not only exists but also is extremely efficient and operates at a frequency substantially above the non-relativistic gyrofrequency. Only the main features of the analysis will be outlined here; the details are currently under study and will be reported soon in a comprehensive publication.

Physical Basis

Generally, in the ECM the motion of the beam electrons is controlled by a simple invariant,<sup>7,8</sup>

$$p = \gamma(n - \beta_{||}) \quad (1)$$

where  $\gamma mc^2$  is the total particle energy,  $\beta_{||} c$  is the axial velocity and  $n = kc/\omega$  is the refractive index for a wave with transverse field polarization, frequency  $\omega$  and wavenumber  $k$ . The invariance of  $p$  is easily seen by comparing  $d\gamma/dt \propto \underline{v}_{\perp} \cdot \underline{E}_{\perp}$  and  $d(\gamma\beta_{||})/dt \propto \hat{e}_{||} \cdot (\underline{v}_{\perp} \times \underline{B}_{\perp})$ , where the wave fields are interrelated by  $\underline{B}_{\perp} = n \hat{e}_{||} \times \underline{E}_{\perp}$ . For  $p$  to be invariant it is required only that  $n$  be constant, that the magnetostatic field  $\underline{B}_0 = B_0 \hat{e}_{||}$  be uniform, and that no axial electric field be present  $\hat{e}_{||} \cdot \underline{E} = 0$ .

Eq. (1) describes trajectories in  $(\gamma, \beta_{||})$  coordinates. These trajectories are given by the hyperbolas  $\gamma = p/(n - \beta_{||})$  with pole at  $\beta_{||} = n$ . Which segment of these hyperbolas is an actual trajectory depends on the full set of equations of motion and depends on the field amplitudes. It is clear however that  $\gamma$  is restricted to values at least equal to  $(1 - \beta_{||}^2)^{-1/2}$ , the value of  $\gamma$  that corresponds to vanishing transverse velocity,  $\beta_{\perp} = 0$ . It can be seen in Fig. 1a that if a fast-wave ( $n < 1$ ) is employed, then only one point with  $\beta_{\perp} = 0$  is present on each hyperbola

$\gamma = p/(n - \beta_{||})$ , and this point corresponds to the minimum energy. Thus, a fast-wave ECM device, such as the gyrotron, requires a beam with transverse energy, which would be converted to radiation energy. On the other hand, in the slow-wave case ( $n > 1$ ) of Fig. 1b each hyperbola  $\gamma = p/(n - \beta_{||})$  intersects the curve  $\gamma = (1 - \beta_{||}^2)^{-1/2}$  at two points, provided that  $p^2 > n^2 - 1$ . One of these points corresponds to maximum energy. Thus, it is seen that it is in principle possible to extract energy from the beam, if the beam is injected exclusively axially, with an initial energy given by the largest root of  $p/(n - \beta_{||}) = (1 - \beta_{||}^2)^{-1/2}$ . Such injection parameters are

$$\gamma_0 = \frac{h + np}{n^2 - 1} \quad (2)$$

$$\beta_{||0} = n - \frac{p}{\gamma_0}, \quad \beta_{\perp 0} = 0,$$

where  $h = (p^2 + 1 - n^2)^{1/2}$ .

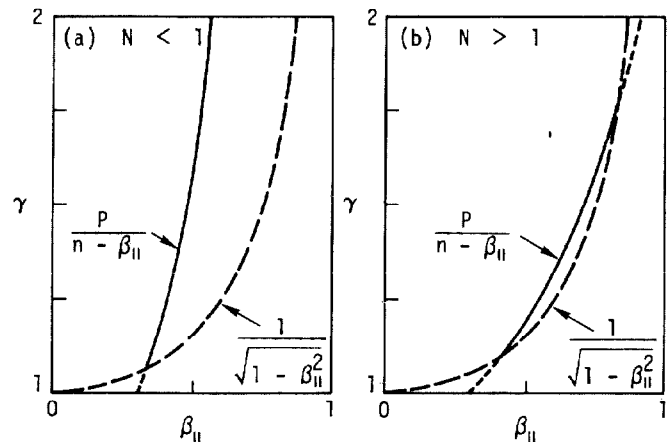


Figure 1. Electron trajectories with  $p$  invariant in coordinates  $(\gamma, \beta_{||})$ , (a) for  $n < 1$ , and (b) for  $n > 1$ . The intersection with the dashed curve  $\gamma = (1 - \beta_{||}^2)^{-1/2}$  gives the points with  $\beta_{\perp} = 0$ .

At first look it might seem paradoxical that a wave with transverse electric field polarization could possibly extract energy from a beam with exclusively

axial velocity. However, it should be remembered that  $\beta_{\perp} = 0$  applies only initially. After a short time interval,  $\Delta t$ , some transverse momentum

$$\Delta(\gamma\beta_{\perp}) = - (e/mc^2)(c\vec{E}_{\perp} + \vec{v}_{\parallel} \times \vec{B}_{\perp})\Delta t = (e/mc) \times (n\beta_{\parallel} - 1)E_{\perp}\Delta t \text{ is developed.}$$

The injection values of Eqs. (2) give  $n\beta_{\parallel} - 1 > 0$ , hence the generated transverse velocity is coparallel with and does work on the wave electric field. How much energy is subsequently converted and how high a conversion efficiency should be expected are questions to be answered from a consideration of the complete set of equations of motion. These questions are addressed and answered in the remainder of this letter.

To study the motion of the electrons, with or without axial injection, a simple model is adopted, in which the wave fields have constant amplitude and circular polarization and are expressed by the vector potential

$$\vec{A} = A [\hat{e}_x \cos\phi + \hat{e}_y \sin\phi], \quad (3)$$

with constant amplitude  $A$  and phase  $\phi = kz - \omega t$ . The magnetostatic field is uniform,  $\vec{B}_0 = B_0 \hat{e}_z$ , while transverse electron velocity is expressed as

$$\vec{v}_{\perp} = \beta_{\perp} c [\hat{e}_x \cos(\phi + \chi) + \hat{e}_y \sin(\phi + \chi)], \quad (4)$$

where  $\chi$  is the azimuthal phase in excess of  $\phi$ . Given the invariance of  $p$ , it suffices to consider the evolution of  $\chi$  and any function of  $\gamma$ . As such function the quantity  $\psi$  is chosen, where

$$\sin \psi \equiv \frac{(n^2 - 1)\gamma - np}{h} \quad (5)$$

The values  $\psi = \pm\pi/2$  correspond to the largest and smallest values of  $\gamma$ , those with  $\beta_{\perp} = 0$ . From the equation of motion, the equations of  $\chi$  and  $\psi$  are obtained. These equations possess an additional integral of the motion, given by

$$K = \sin^2\psi - C_B \sin\psi + C_A \cos\psi \cos\chi. \quad (6)$$

where  $C_A = 2(eA/cm^2) h^{-1} \sqrt{n^2 - 1}$ ,  $C_B = (\Omega/\omega)h^{-1}$ , and  $\Omega = eB_0/mc$ . This constant can be used to reduce the problem to a quadrature and to describe the motion of each individual electron in terms of elliptic functions. The procedure is beyond the point at present. The most important use of  $K$  is that  $K(\psi, \chi) = \text{const}$  describes the actual trajectories in phase space  $(\psi, \chi)$ .

Of particular interest is the curve  $K(\psi, \chi) = K_0 = 1 - C_B$ , which passes through the point  $\psi = \pi/2$ , i.e., the point with maximum energy and  $\beta_{\perp} = 0$ . Phase space trajectories with  $K_0 = 1 - C_B$  are given in Fig. 2 for  $C_B = 1$  and various values of  $C_A$ . In this figure the horizontal axis is limited to the interval  $0 < \chi < \pi$ , in which the electron transverse velocity is at an acute angle relative to  $E_{\perp}$  and the electrons lose energy ( $d\psi/dz < 0$ ). For small values of  $C_A$ , both  $\chi$  and  $\psi$  decrease, until a minimum value  $\psi_{\min}$  is reached  $\chi = 0$ . Subsequently,  $\psi$  again increases with  $\chi < 0$ . This segment of the trajectory is symmetric about  $\chi = 0$  to the segment shown. Given the linear relationship between  $\gamma$  and  $\sin\psi$  in Eq. (5), the maximum energy  $\Delta\gamma$  lost by the

electron is proportional to  $1 - \sin\psi_{\min}$ . It can be seen that  $\Delta\gamma$  increases with  $C_A$  but generally remains small, until  $C_A$  reaches a critical value (just in excess of 0.3 in this case). For values of  $C_A$  exceeding this critical value, it is  $\chi$  that first reaches a minimum value  $\chi_{\min}$ , beyond which it starts increasing, while  $\psi$  continuously decreases up to  $\psi_{\min}$  at  $\chi = \pi$ . The continuation of this curve is symmetric about  $\chi = \pi$ , with  $\psi$  increasing. For these larger values of  $C_A$  the energy lost by the electrons is substantially higher than before, due to the discontinuity at the critical value  $C_{Acrit}$ .

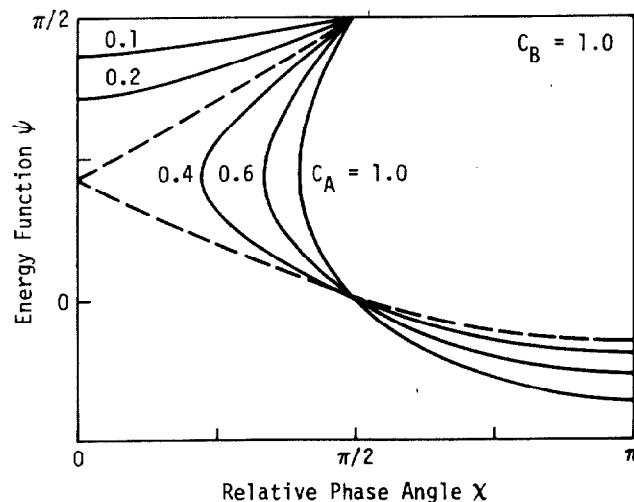


Figure 2. Electron trajectories in phase space  $(\psi, \chi)$  for electrons starting with  $\beta_{\perp 0} = 0$ ,  $\gamma_0 = \gamma_{\max}$ , for  $C_B = 1$  and  $C_A = \text{as shown}$ . The dashed curve corresponds to the values of  $C_A$  at transition from low to high efficiency.

#### Efficiency

The foregoing discussion bears direct relevance to the efficiency of the interaction. The efficiency is equal to the fraction of initial beam power converted to electromagnetic power. With consideration for the conservation of particle flux in steady state, the efficiency is given by  $\eta = \langle \gamma_0 - \gamma_f \rangle / \langle \gamma_0 - 1 \rangle$ , where  $\gamma_f$  is the final value of  $\gamma$  and the angular brackets represent an ensemble average over all beam electrons. In general, the efficiency can be written as the product  $\eta = \eta_1 \eta_2$ , where  $\eta_1$  is the fraction of the available to the interaction and  $\eta_2$  is the fraction of the available energy that is actually lost by the beam. In the present configuration of an axially injected monoenergetic beam, the efficiency  $\eta_1 = 2h/(1 + h + np - n^2)$  can be maximized to  $\eta_1 = 1$  by requiring that  $h = 1$  (i.e.,  $p = n$ ). On the other hand, the efficiency  $\eta_2$  is

$$\eta_2 = \frac{1 - \sin\phi_f}{2}. \quad (7)$$

No ensemble averaging is involved, since the electrons are not distinguished in their initial phase angle  $\chi_0$ . The interaction length can be optimized, so that  $\psi_f = \psi_{\min}$ . The resulting optimized efficiency is a function of  $C_A$  and  $C_B$  and is presented in Fig. 3. In this figure the regions of high and low efficiency are distinguished. As has already been discussed, the high efficiency region occurs for sufficiently large  $C_A$  and  $C_B$  and is the result of the occurrence of  $\psi_{\min}$  at  $\chi = \pi$ , while the opposite holds for the low efficiency region. The boundary of these two regions is given by the dashed curve in Fig. 3.

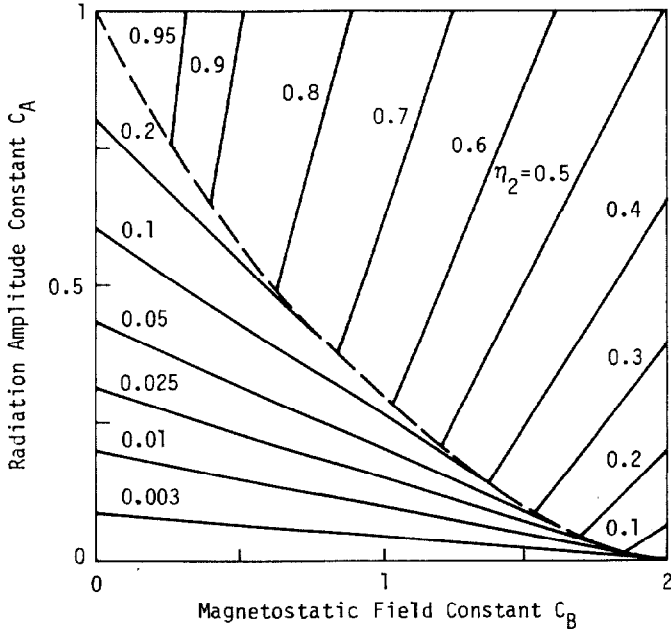


Figure 3. Efficiency  $\eta_2$  as function of  $C_A$  and  $C_B$  for optimized interaction length and axial beam injection. The dashed curve separates the low and high efficiency regions.

As can be seen in Fig. 3, the efficiency  $\eta_2$  approaches the value  $\eta_2 = 100$  percent for  $C_B \rightarrow 0$  and  $C_A \rightarrow 1$ . In practice, such an operation is not expected to be feasible, primarily because it requires  $B_0 = 0$ , while a finite value of  $B_0$  is necessary to confine the nonneutralized electron beam. In addition,  $C_A = 1$  corresponds to relatively high values of the radiation fields. It appears to be more convenient to design this maser to operate with  $C_B \sim 1$ . In this domain, relatively moderate values  $C_A \sim 0.5$  give enormous efficiencies  $\eta_2$ , well in excess of 50 percent. In choosing the design value of  $C_A$ , care must be taken to take it somewhat larger than the critical value, to avoid potential difficulties when the electrons pass in the vicinity of the saddle point.

#### Examples

To demonstrate the potential of this interaction, several conceptual designs are presented in Table 1. For these designs the values  $C_A = 0.41$  and  $C_B = 1$  have been chosen, giving an efficiency  $\eta_2 = 0.65$  for

optimized interaction length. As an additional constraint, the radiation electric field has been taken to satisfy  $E_{\perp} \lambda_{fs} = 100$  kV, where  $\lambda_{fs} = 2\pi c/\omega$  is the free space wavelength of the radiation. This leaves one free parameter. As such is chosen the square of the refractive index, which is equal to the effective dielectric constant of the propagation structure. It is seen in the examples of Table 1 that this maser can operate with both relativistic and mildly relativistic electron beams, with a high efficiency, approximately 50 percent higher than the gyrotron. (For a fair comparison, it is necessary to consider the gyrotron without optimization of the axial distribution of the radiation and magnetostatic fields.) An additional attractive feature of this interaction is the low magnetostatic field it needs. In the examples of Table 1 the magnetostatic field is 2.5 to 36 times weaker than what is required for the gyrotron, for which  $\Omega \approx \gamma_0 \omega$ .

Table 1. Design examples for  $C_A = 0.41$ ,  $C_B = 1$  and  $E \lambda_{fs} = 100$  kV

Refractive Index Squared $n^2[-]$	Initial Beam Energy $\epsilon_b[\text{keV}]$	Normalized Gyrofrequency $\Omega/\omega[\%]$	Efficiency $\eta[\%]$
1.5	494	5.4	29.0
2.0	298	7.6	34.0
4.0	131	13.2	44.7
8.0	71	20.2	53.9
15.0	45	28.5	60.2
30.0	29	41.0	64.4

Due to its preliminary nature, this letter has not addressed issues like the calculation of the optimized interaction length, the effects of thermal spreads, the small-signal evolution, the competition of this interaction with the conventional Cherenkov interaction, etc. These issues will be addressed in the comprehensive manuscript currently in preparation.

The author wishes to acknowledge constructive discussions with Y. Carmel, K. R. Chu, F. S. Felber, V. L. Granatstein, M. E. Read, and C. Roberson. This work was supported in part by DARPA through the Naval Surface Weapons Center.

#### References

1. J.L. Hirshfield, I.B. Bernstein, and J.B. Wachtel, IEEE J. Quantum Electron. **QE-1**, 237 (1965).
2. P. Sprangle and A.T. Drobot, IEEE Trans. Microwave Theory Tech. **MTT-25**, 528 (1977).
3. K.R. Chu, Phy. Fluids **21**, 2354 (1978).
4. H. Jory, S. Hegji, J. Shiverly, and R. Symons, Microwave J. **21**, 30 (1978).
5. A.V. Gaponov, V.A. Flyagin, A.L. Gol'denberg, G.S. Nusinovich, Sh.E. Tsimring, V.G. Usov, and S.N. Vlasov, Int. J. Electron. **51**, 277 (1981).
6. K.J. Kim, M.E. Read, J.M. Baird, K.R. Chu, A. Brobot, J.L. Vomvoridis, A. Ganguly, D. Dialetis, and V.L. Granatstein, Int. J. Electron. **51**, 427 (1981).
7. J.L. Vomvoridis and P. Sprangle, Phys. Rev. A **25**, 931 (1982).
8. J.L. Vomvoridis, Int. J. Electron. **53**, in press (1982).